


# Comprehensive microRNA expression analysis of pediatric gonadal germ cell tumors: unveiling novel biomarkers and signatures

Ana Glenda Santarosa Vieira<sup>1,2,3</sup> , Luciane Sussuchi da Silva<sup>4</sup>,  
Eduardo Caetano Albino da Silva<sup>5</sup>, Ana Carolina Laus<sup>4</sup>, Thaïssa Maria Veiga Faria<sup>1</sup>,  
André van Helvoort Lengert<sup>4</sup>, Gisele Eiras Martins<sup>1,2</sup>, Marco Antônio de Oliveira<sup>4</sup>,  
Rui Manuel Reis<sup>4,6,7</sup>, Luiz Fernando Lopes<sup>1,2</sup> and Mariana Tomazini Pinto<sup>4,8</sup>

1 Barretos Children's Cancer Hospital from Hospital de Amor, Brazil

2 Brazilian Childhood Germ Cell Tumor Study Group, The Brazilian Pediatric Oncology Society (SOBOPE), São Paulo, Brazil

3 Pediatric Cancerology's Department of Santa Casa de Misericórdia de Santos, Brazil

4 Molecular Oncology Research Center, Barretos Cancer Hospital, Brazil

5 Department of Pathology, Barretos Cancer Hospital, Brazil

6 Life and Health Sciences Research Institute (ICVS), Medical School, University of Minho, Braga, Portugal

7 ICVS/3B's-PT Government Associate Laboratory, Braga, Portugal

8 Pediatric Oncology Research Group (GPOPed), Molecular Oncology Research Center, Barretos Cancer Hospital, Brazil

## Keywords

biomarkers; germ cell tumor; microRNA;  
ovarian cancer; pediatric cancer; testicular  
cancer

## Correspondence

A. G. Santarosa Vieira, Barretos Children's  
Cancer Hospital from Hospital de Amor;  
Pediatric Cancerology's Department of  
Santa Casa de Misericórdia de Santos,  
Avenida Dr. Claudio Luiz da Costa, 50, CEP  
11075101, Santos, São Paulo, Brazil  
E-mail: [santarosacontact@draanaglenda.com.br](mailto:santarosacontact@draanaglenda.com.br);  
[anaglendaoncoped@gmail.com](mailto:anaglendaoncoped@gmail.com)  
and

M. Tomazini Pinto, Molecular Oncology  
Research Center, Barretos Cancer Hospital,  
Rua Antenor Duarte Villela, 1331, CEP 14784-  
400. Barretos, São Paulo, Brazil  
E-mail: [marianatomazini@yahoo.com](mailto:marianatomazini@yahoo.com); [mariana.pinto49@edu.hospitaldeamor.com.br](mailto:mariana.pinto49@edu.hospitaldeamor.com.br)

(Received 1 September 2023, revised 11  
December 2023, accepted 15 February  
2024, available online 9 May 2024)

doi:10.1002/1878-0261.13617

microRNAs (miRNAs) are small endogenous noncoding RNAs, and alterations in their expression may contribute to oncogenesis. Discovering a unique miRNA pattern holds the potential for early detection and novel treatment possibilities in cancer. This study aimed to evaluate miRNA expression in pediatric patients with gonadal germ cell tumors (GCTs), focusing on characterizing the miRNA profiles of each histological subtype and identifying a distinct histological miRNA signature for a total of 42 samples of pediatric gonadal GCTs. The analysis revealed distinct miRNA expression profiles for all histological types, regardless of the primary site. We identified specific miRNA expression signatures for each histological type, including 34 miRNAs for dysgerminomas, 13 for embryonal carcinomas, 25 for yolk sac tumors, and one for immature teratoma, compared to healthy controls. Furthermore, we identified 26 miRNAs that were commonly expressed in malignant tumors, with six miRNAs (miR-302a-3p, miR-302b-3p, miR-371a-5p, miR-372-3p, miR-373-3p, and miR-367-3p) showing significant overexpression. Notably, miR-302b-3p exhibited a significant association with all the evaluated clinical features. Our findings suggest that miRNAs have the potential to aid in the diagnosis, prognosis, and management of patients with malignant GCTs.

## Abbreviations

AFP, alpha-fetoprotein; AUC, area under the ROC curve; CC, choriocarcinoma; COG, Classification of The Children's Oncology Group; EAU, European Association of Urology; EC, embryonal carcinoma; FC, fold change; FFPE, formalin-fixed paraffin-embedded; FIGO, Classification of The International Federation of Gynecology and Obstetrics; GCTs, germ cell tumors; H&E, hematoxylin and eosin; HCG, human chorionic gonadotropin; IT, immature teratoma; LDH, lactic dehydrogenase; miRNA, microRNA; mRNAs, messenger RNAs; NSGCTs, nonseminomatous germ cell tumors; QC, quality controls; ROC, receiver operating characteristic curve; TGCT, testicular germ cell tumor; T-SNE, t-distributed stochastic neighborhood embedding; WHO, World Health Organization; YST, yolk sac tumor.

## 1. Introduction

Germ cell tumors (GCTs) encompass a spectrum of benign or malignant neoplastic diseases that differ significantly in their clinical presentation, histology, and biological behavior [1,2]. Among childhood tumors, GCTs are rare, accounting for approximately 3% of cases, and may arise either in gonadal or extragonadal sites [3].

Malignant GCTs are divided into seminomatous and nonseminomatous (NSGCTs). Seminomatous GCTs, resembling undifferentiated germ cells, are rare in young children and are more common in adolescents and young adults. Nonseminomatous GCTs can be further divided into different histologies, including embryonal carcinoma (EC), yolk sac tumor (YST), choriocarcinoma (CC), and immature teratoma (IT). Mature teratomas are generally benign and are characterized by well-differentiated tissue. GCTs often exhibit mixed histology, encompassing EC, YST, CC, and teratoma components [4].

GCT diagnosis includes a physical examination, imaging modalities, and measurement of serum biomarkers [5]. A set of serum biomarkers are informative for diagnosis, risk assessment, and follow-up, including alpha-fetoprotein (AFP), human chorionic gonadotropin (HCG), and lactic dehydrogenase (LDH) [6]. AFP is primarily informative for YST with sporadic positivity in EC, while HCG is mainly informative for CC with sporadic positivity in EC [7]. LDH has been described as a serum marker of disease severity rather than a specific histological type [8]. Teratomas typically present absence in AFP and/or HCG serum levels [7]. However, none of these markers are specific for GCTs and may be expressed in other tumors such as hepatoblastoma, as well as non-oncological conditions such as anatomical neural tube defect and diabetes, limiting their diagnostic and follow-up utility. Therefore, more specific biomarkers are needed for accurate diagnosis, prognosis, and therapy monitoring in pediatric GCTs [6,9]. Exploring miRNA signatures adapted to each GCT histological subtype is crucial.

microRNAs (miRNAs) are small endogenous non-coding RNAs consisting of 18–25 nucleotides [10]. MiRNAs play an important role in post-transcriptional regulation by cleaving or repressing the translation of target messenger RNAs (mRNAs). Alterations in expression may contribute to oncogenesis by affecting cell proliferation, differentiation, and apoptosis, suggesting that miRNA alteration may lead to oncogenesis [11,12].

Previous investigations have identified miRNAs associated with the tumorigenesis of GCTs. Palmer

et al. [13] reported the overexpression of six miRNAs in malignant GCTs compared to normal tissues, demonstrating the association of these miRNAs with histological (YST/EC/seminoma), primary location (gonadal/extragenital), and patient age (pediatric/adult). Syring et al. [14] found that serum levels of miRNAs were elevated in patients with testicular GCT (TGCT) and reported that the miR-371a-3p specifically outperformed HCG or AFP assays, suggesting the potential clinical utility of this miRNA in the management of TGCT patients. Furthermore, serum levels of miR-371a-3p presented superior performance compared to conventional markers (AFP, HCG, and LDH) [15].

Despite these studies, limited information is available regarding miRNA profiles that can distinguish between histological types of pediatric GCTs. Therefore, this study aimed to evaluate the miRNA expression in pediatric patients with gonadal GCTs, focusing on characterizing the miRNA profiles of each histological subtype and identifying a distinctive histological miRNA signature for pediatric gonadal GCTs.

## 2. Materials and methods

### 2.1. Study population and sample collection

This retrospective cohort study analyzed 42 pediatric gonadal GCT patients who were treated at Barretos Children's Cancer Hospital (Brazil), between 2000 and 2017. It included 31 GCT ovarian tumors and 11 testicular GCT (TGCT). Based on staining with hematoxylin and eosin (H&E), the slides from the paraffin block of each tumor resected at diagnosis had the tumor area delimited by the experienced pathologist to isolate the tumor material. Initially, a 5 micron cut was made in each paraffin block for H&E staining in order to delimit the tumor tissue. Next, five 10-micron sections were made to be used in RNA extraction and, at the end, a new 5-micron section was stained with H&E so that the pathologist could assess the permanence of the tumor in the previous sections. As a control group, we used non-tumoral tissue adjacent to the tumors from 10 pediatric GCT patients. The classification of GCTs was determined according to the 2016 World Health Organization (WHO) guidelines. The risk of treatment was determined by risk stratification according to tumor stage. Stage I gonadal tumors were classified as low-risk and were treated with surgery alone, without adjuvant chemotherapy. Stages II, III,

and IV in patients younger than 11 years were classified as intermediate-risk and received two chemotherapeutic agents (cisplatin and etoposide) for a total of four cycles. Stage IV gonadal tumors in patients aged 11 years or older were classified as high-risk and received a total of five cycles of three chemotherapeutic agents (cisplatin, etoposide, and ifosfamide) and were followed up regularly with imaging and serologic markers [16].

Sociodemographic and clinicopathological data were retrospectively collected from medical records. This study was approved by the local ethics committee (Barretos Cancer Hospital IRB/Project No. 1692/2018). Due to the great difficulty in locating the participants to consent to them, even considering that a portion of this population has already died, the CEP-HCB exempted the study from the application of the ICF based on if in your right by resolution 466/2012, believing that we could cause great emotional suffering for the family, in addition to being a retrospective study, which used only slides and paraffin blocks already stored in the pathology sector of the Barretos Cancer Hospital and consultation in medical records.

## 2.2. RNA isolation

RNA isolation was performed from formalin-fixed paraffin-embedded (FFPE) tumor samples, sectioned on slides with a thickness of 10  $\mu\text{m}$  as previously reported [17]. Based on hematoxylin and eosin (H&E) staining, the area of tumor tissue was selected by an experienced pathologist for isolation of tumor material, containing at least 70% of the tumor area. RNA was isolated using the *RecoverAll Total Nucleic Acid Isolation Kit* (Thermo Fisher Scientific, Waltham, MA, USA), according to the manufacturer's instructions. The purity and quantification of total RNA were assessed using a ND-1000 NanoDrop spectrophotometer (Thermo Fisher Scientific) and a Qubit 2.0 instrument (Thermo Fisher Scientific).

## 2.3. NanoString nCounter system for miRNA expression assessment

The expression of approximately 800 human miRNAs was measured using the Human v3 miRNA Assay CSO Panel (CSO-MIR3-12, NanoString Technologies, Seattle, WA, USA) with the nCounter Analysis System technology (NanoString Technologies) as previously reported [18]. Sample preparation, hybridization, detection, and scanning procedures were performed according to the instructions of NanoString Technologies (NanoString). Briefly, total RNA (100 ng),

quantified by Qubit Fluorometer System (Thermo Fisher Scientific), was initially submitted to the miRNA tag ligation reaction, followed by hybridization with Capture and Reporter Probes for 21 h at 65 °C. The purification and immobilization of probe-target complexes were performed in the nCounter PrepStation System and the cartridges were analyzed in nCounter Digital Analyzer (NanoString), which captures up to 555 fields of view per sample. Standardized quality controls (QC) were performed using NSOLVER SOFTWARE (NanoString) for all samples, including imaging QC, binding density, limit of detection, positive controls linearity, and negative control levels. All samples that met quality control criteria were eligible for data analysis. Data analysis was performed using R v4.1.2 (The R Foundation, Vienna, Austria) with the NANOSTRINGNORM package v 1.2.1.1 [19,20]. Evaluated miRNAs were considered not expressed if their raw expression level was below the mean plus five times the standard deviation of the negative controls in all samples. Normalization of samples was performed using the quantile method and  $\log_2$  transformation, followed by differential expression and statistical analysis. For differential expression, a two-fold change (FC) difference in miRNA expression levels and a significance level of Bonferroni-corrected  $P$ -value  $\leq 0.05$  were adopted.

## 2.4. Statistical analysis

Heatmaps and clustering of differentially expressed genes were generated with the COMPLEX HEATMAP R package v2.12.1 [18] using Pearson's correlation distance. The R implementation of t-distributed stochastic neighbor embedding [21,22] in the RTSNE package v0.15 was applied to visualize the histological subgroups of GCTs. Boxplots of gene expression levels and Kruskal–Wallis tests were created using the GGPUBR package v0.4.0.

Statistical analyses associated with clinical factors were performed using the IBM-SPSS software program for Windows/Mac, version 23.0 (SPSS Inc, Chicago, IL, USA). A  $P$ -value  $\leq 0.05$  was considered statistically significant.

Samples were characterized using frequency tables for qualitative variables, and central tendency (mean, median) and dispersion (standard deviation, minimum, and maximum) were measured for quantitative variables.

The Student's  $t$ -test or Mann–Whitney test was performed after verification of normality, which was tested by the Kolmogorov–Smirnov test. The ROC curve analysis was performed using the ROCR package v1.0-11 [21]. MicroRNAs presenting an area under the

ROC curve (AUC)  $\geq 0.75$  were considered to have a good performance.

### 3. Results

#### 3.1. Clinicopathologic features of pediatric GCT patients

The clinicopathologic features of the 42 patients are summarized in Table 1. Most patients had ovarian tumors ( $n = 31$ , 73.8%), and 11 patients (26.2%) had testicular tumors. The average age at diagnosis was 11.8 years (range, 0–19 years), with females 14.1 years and males 5.4 years old. Clinical findings showed that 26.2% of patients (11/42) had yolk sac tumors, followed by 16.7% mature teratomas and 9.5% embryonal carcinomas. Among female patients, 16% (5/31) had immature teratomas and 42% had dysgerminomas (13/31), while among male patients, 18.2% (2/11) had prepubertal teratomas.

Around half of the patients were classified as low-risk (50%) and had early stages (FIGO I/COG I) (48.3%), and 23.8% (10/42) had metastases at diagnosis. Half of the patients were treated with chemotherapy, a minority had tumor recurrence (12%), and 92.8% were still alive.

#### 3.2. microRNA expression signature of the individual histological types of GCTs

All 42 cases showed reliable miRNA analysis. Initially, we examined the miRNA profiles of both ovarian and testicular tumors. As expected, we found that mature teratomas clustered with healthy controls (Fig. S1). Subsequently, we examined the miRNA profiles of malignant tumors of both sites individually. The miRNA expression profile of each histology was compared with healthy controls to identify differentially expressed miRNAs for each histological type (Fig. 1 and Fig. S2).

We identified 91 differentially expressed miRNAs in dysgerminomas compared to healthy controls, with 34 specific to this histological subtype, of which 30 miRNAs were upregulated and four downregulated (Table S1). Fifty-four miRNAs were differentially expressed between the embryonal carcinoma and controls, with 13 being specific to EC. Among these 13 miRNAs, one was upregulated and 12 were downregulated (Table S2). Yolk sac tumors showed 80 differentially expressed miRNAs compared to healthy controls. Among these, 25 miRNAs were specific to YST, with 20 upregulated and five downregulated (Table S3). When immature teratomas were compared with healthy controls, we observed 13 differentially expressed miRNAs,

**Table 1.** Clinicopathologic features of GCTs in pediatric patients. COG, classification of The Children's Oncology Group; DP, standard deviation; FIGO, classification of The International Federation of Gynecology and Obstetrics.

Features	Total, n (%)	Ovary, n (%)	Testis, n (%)
N (%)	42 (100)	31 (73.8)	11 (26.2)
Average age (years)	11.8 (5.4)	14.1 (2.9)	5.4 (6.0)
Histology			
Yolk sac tumor	11 (26.2%)	4 (13%)	7 (63.6%)
Embryonal carcinoma	4 (9.5%)	2 (6.5%)	2 (18.2%)
Mature teratoma	7 (16.7%)	7 (22.5%)	–
Immature teratoma	5 (11.9%)	5 (16%)	–
Morris grade I	1	1	–
Morris grade II	2	2	–
Morris grade III	2	2	–
Prepubertal testicular teratoma	2 (4.7%)	–	2 (18.2%)
Postpubertal testicular teratoma	0	–	0
Dysgerminoma/Seminoma	13 (31%)	13 (42%)	0
Staging			
FIGO classification			
I	15	15 (48.3%)	–
II	4	4 (13%)	–
III	10	10 (32.2%)	–
IV	2	2 (6.5%)	–
COG classification			
I	13	5 (16.1%)	8 (72.8%)
II	12	11 (35.5%)	1 (9%)
III	13	13 (41.9%)	0 (0)
IV	4	2 (6.5%)	2 (18.2%)
Risk			
Low	21 (50%)	13 (41.9%)	8 (72.8%)
Intermediate	8 (19%)	7 (22.6%)	1 (9%)
High	13 (31%)	11 (35.5%)	2 (18.2%)
Metastasis			
Yes	10 (23.8%)	7 (22.5%)	3 (27.3%)
No	32 (76.2%)	24 (77.5%)	8 (72.7%)
Chemotherapy			
Yes	21 (50%)	18 (58%)	3 (27.3%)
No	21 (50%)	13 (42%)	8 (72.7%)
Relapse			
Yes	5 (12%)	2 (6.5%)	3 (27.3%)
No	37 (88%)	29 (93.5%)	8 (72.7%)
Status			
Alive	39 (92.8%)	29 (93.5%)	10 (91%)
Dead	3 (7.2%)	2 (6.5%)	1 (9%)

of which only one (miR-199b-5p) ( $P_{\text{adj}} = 0.0013$  and  $\log_2$  fold change of 3.1) was upregulated and specific for immature teratomas.

The t-distributed stochastic neighborhood embedding (T-SNE) algorithm was further used to visualize the classification of different histological types of GCTs based on the normalized expression of the

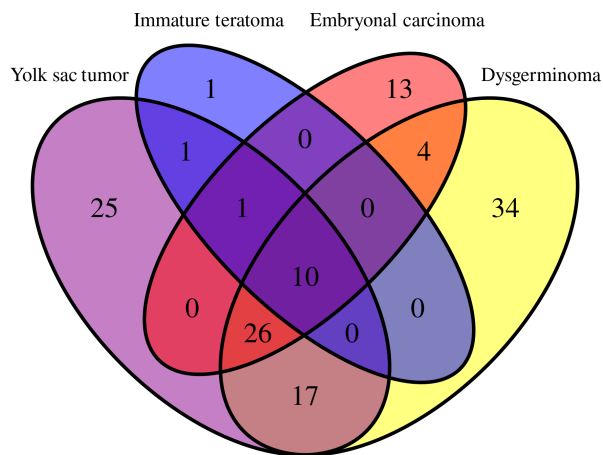


**Fig. 1.** Venn diagram shows miRNA distribution among the different GCT histologies. Venn diagrams indicating the number of significant differentially expressed miRNAs in embryonal carcinomas (13 miRNAs), dysgerminomas (34 miRNAs), yolk sac tumors (25 miRNAs), and immature teratomas (1 miRNA), and the overlap regions showing the number of miRNAs that are expressed in two or more histologies.

histology-specific miRNA (Fig. 2). Our results show each histological type expressing a specific miRNA signature.

### 3.3. Overlap of differentially expressed miRNAs in pediatric malignant tumor samples

To analyze the similarity of miRNA expression among the different malignant histological types, we evaluated their overlap. The analysis revealed a total of 132 unique differentially expressed miRNAs across the four malignant histological types (Fig. 1). Only hsa-miR-205-5p showed an overlap between YST and IT. The hsa-miR-200b-3p was common to YST, IT, and EC, while four miRNAs showed an overlap between EC and dysgerminoma (miR-1246, miR-135a-5p, miR-140-5p, and miR-342-3p). In addition, 17 miRNAs were common to dysgerminomas and YST (let-7b-5p, miR-10b-5p, miR-130a-3p, miR-150-5p, miR-1915-3p, miR-194-5p, miR-199a-3p + hsa-miR-199b-3p, miR-199a-5p, miR-23b-3p, miR-25-3p, miR-302c-3p, miR-302d-3p, miR-509-5p, miR-514b-5p, miR-596, miR-7-5p, and miR-93-5p).

Among all malignancies, 10 miRNAs in common were downregulated when compared to normal tissues, including miR-195-5p, miR-29a-3p, miR-497-5p, miR-503-5p, miR-506-3p, miR-507, miR-509-3p, miR-513b-5p, miR-513c-5p, and miR-514a-3p. The analysis also revealed an overlap of 26 miRNAs between YST, EC,

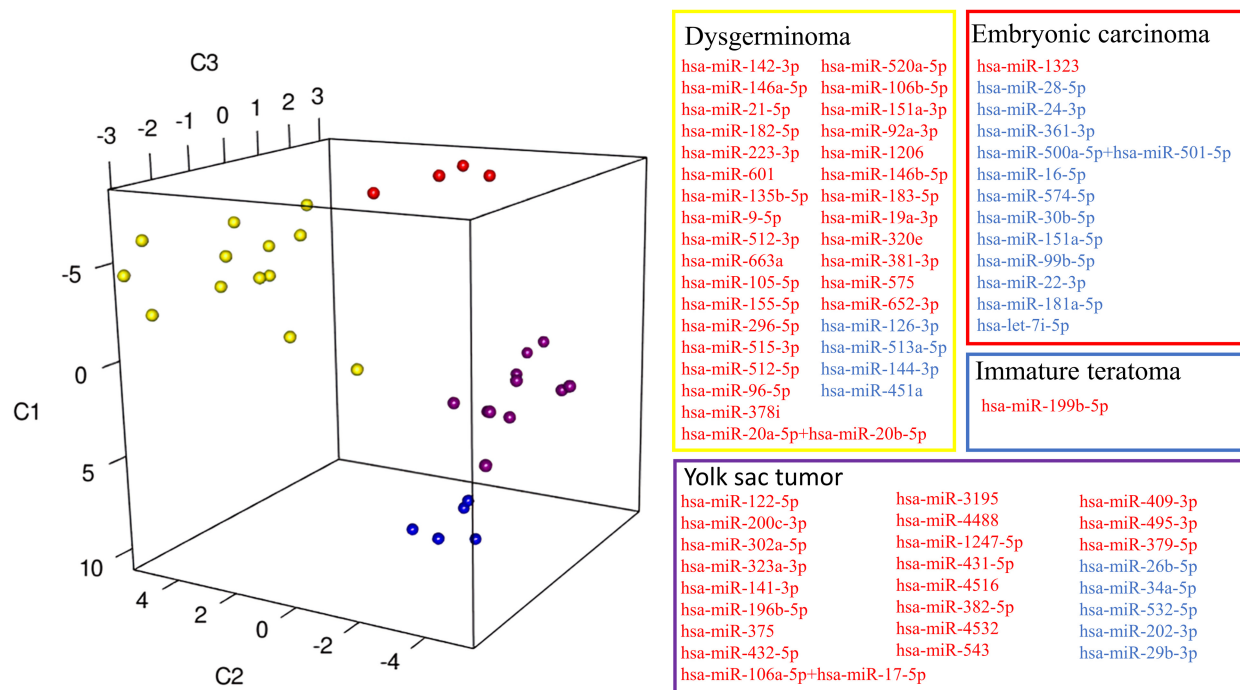


**Fig. 2.** T-SNE visualization of miRNA expression according to GCT histological types. Embryonal carcinoma, yolk sac tumor, dysgerminoma, and immature teratoma express specific signatures of miRNAs. Data points (representing patients) have been color-coded based on their histologies, and miRNAs have been grouped together based on the same histological patterns. Yellow dots indicate dysgerminoma samples, red dots the embryonal carcinoma, purple dots the yolk sac tumors, and blue dots immature teratoma. Blue and red colors indicate the miRNAs with lower and higher expression levels, respectively.

and dysgerminomas, with 20 miRNAs downregulated and six upregulated in tumor tissues (Table 2).

We further compared the six overexpressed miRNAs in malignant GCT (Table 2) across all histologies (Fig. 3). Different histologies showed a distinct profile of miRNA expression. Notably, yolk sac tumors, which are associated with greater tumor aggressiveness, exhibited overexpression of miR-302a-3p and miR302b-3p ( $P \leq 0.001$ ) compared to the other histologies, suggesting that these two miRNAs could be used to evaluate the prognosis of GCT patients.

To further assess the relevance of these six miRNAs, a ROC curve was established, and the AUC was determined (Fig. 4). All six miRNAs exhibited a significant AUC value (1.0), suggesting their significant diagnostic value for discrimination between control and GCT pediatric patients. Further studies with larger sample sizes are necessary to confirm their predictive value.

Next, we analyzed the association of these miRNAs with clinical characteristics, including histology, risk, metastasis, AFP marker before surgery, relapse, and status (Table 3). We observed that miR-302b-3p was the only miRNA significantly associated with all the evaluated parameters, followed by miR-302a-3p, which

showed significant association with all parameters except for metastasis. Due to the small number of cases, it was impossible to perform a survival analysis; however, patients who died had a significantly higher expression of miR-302a-3p ( $P = 0.009$ ) and miR-302b-3p ( $P = 0.036$ ). MiR-367-3p was significantly associated with AFP marker before surgery ( $P = 0.002$ ), and miR-371a-5p was significantly associated with risk ( $P \leq 0.001$ ). No significant associations were observed for miR-372-3p and miR-373-3p.

### 3.4. Identification of differentially expressed miRNAs among pediatric malignant tumors

We found significant clustering of miRNA expression profiles according to histological type (Fig. 5). Two main clusters were observed: (a) YST and immature teratomas and (b) dysgerminomas and EC. The analysis also revealed a clear separation between the different histological subtypes (Fig. 5). In total, we identified 39 miRNAs with differential expression in the malignant tumor samples, namely miR-367-3p and miR-196b-5p were associated with YST; the miR-371~373 cluster, miR142-3p, and miR-146a-5p were associated with

**Table 2.** Overlap of 26 differentially expressed miRNAs in yolk sac tumor, dysgerminoma, and embryonal carcinoma.

miRNAs	Yolk sac tumor		Dysgerminoma		Embryonal carcinoma	
	<i>P</i> <sub>adj</sub>	Log <sub>2</sub> fold change	<i>P</i> <sub>adj</sub>	Log <sub>2</sub> fold change	<i>P</i> <sub>adj</sub>	Log <sub>2</sub> fold change
miR-302b-3p	5.2E-11	9.3	9.9E-09	6.4	0.003	7.9
miR-302a-3p	1.6E-10	7.5	2.5E-08	3.8	0.006	6.1
miR-372-3p	2.0E-08	6.5	4.8E-15	7.5	0.00027	6.6
miR-373-3p	2.6E-07	6.0	4.8E-15	7.5	1.0E-07	6.4
miR-367-3p	1.6E-10	5.8	1.3E-05	2.6	0.049	4.9
miR-371a-5p	0.0014	1.8	1.5E-10	3.5	0.0012	3.3
let-7e-5p	0.0046	-1.0	1.1E-05	-1.9	0.003	-3.5
miR-27b-3p	0.00034	-1.0	1.1E-05	-1.3	0.0031	-2.0
miR-214-3p	0.011	-1.1	0.0015	-1.7	0.006	-2.6
let-7d-5p	0.00059	-1.3	6.3E-08	-1.7	0.025	-3.8
let-7f-5p	0.0021	-1.3	0.00086	-1.4	1.1E-06	-3.1
miR-98-5p	3.3E-06	-1.4	1.4E-05	-1.6	3.8E-06	-2.6
miR-26a-5p	0.0023	-1.5	0.025	-1.0	0.0028	-3.0
miR-29c-3p	0.0013	-1.7	0.041	-1.0	0.00052	-3.9
miR-145-5p	0.0021	-1.9	0.00048	-2.2	0.0014	-4.8
let-7a-5p	0.00048	-2.0	0.0041	-1.8	0.035	-10
miR-450a-5p	8.9E-05	-2.0	4.5E-08	-3.1	0.018	-3.3
miR-204-5p	0.013	-2.1	0.00075	-2.9	0.047	-2.3
let-7 g-5p	6.1E-06	-2.2	0.0037	-1.1	0.002	-3.7
miR-509-3-5p	0.0065	-2.5	0.006	-2.6	0.011	-2.9
miR-100-5p	5.6E-07	-2.7	1.5E-05	-1.9	0.0037	-3.8
miR-424-5p	6E-07	-2.8	1.5E-11	-4.4	0.048	-4.8
let-7c-5p	1.5E-05	-3.4	4.4E-09	-3.6	0.000039	-5.3
miR-125b-5p	2.8E-06	-3.5	2.3E-06	-2.7	0.0051	-5.9
miR-99a-5p	6.7E-08	-3.7	9.9E-09	-3.9	0.000039	-5.3
miR-508-3p	0.00051	-4.8	0.00038	-5.1	0.024	-4.4

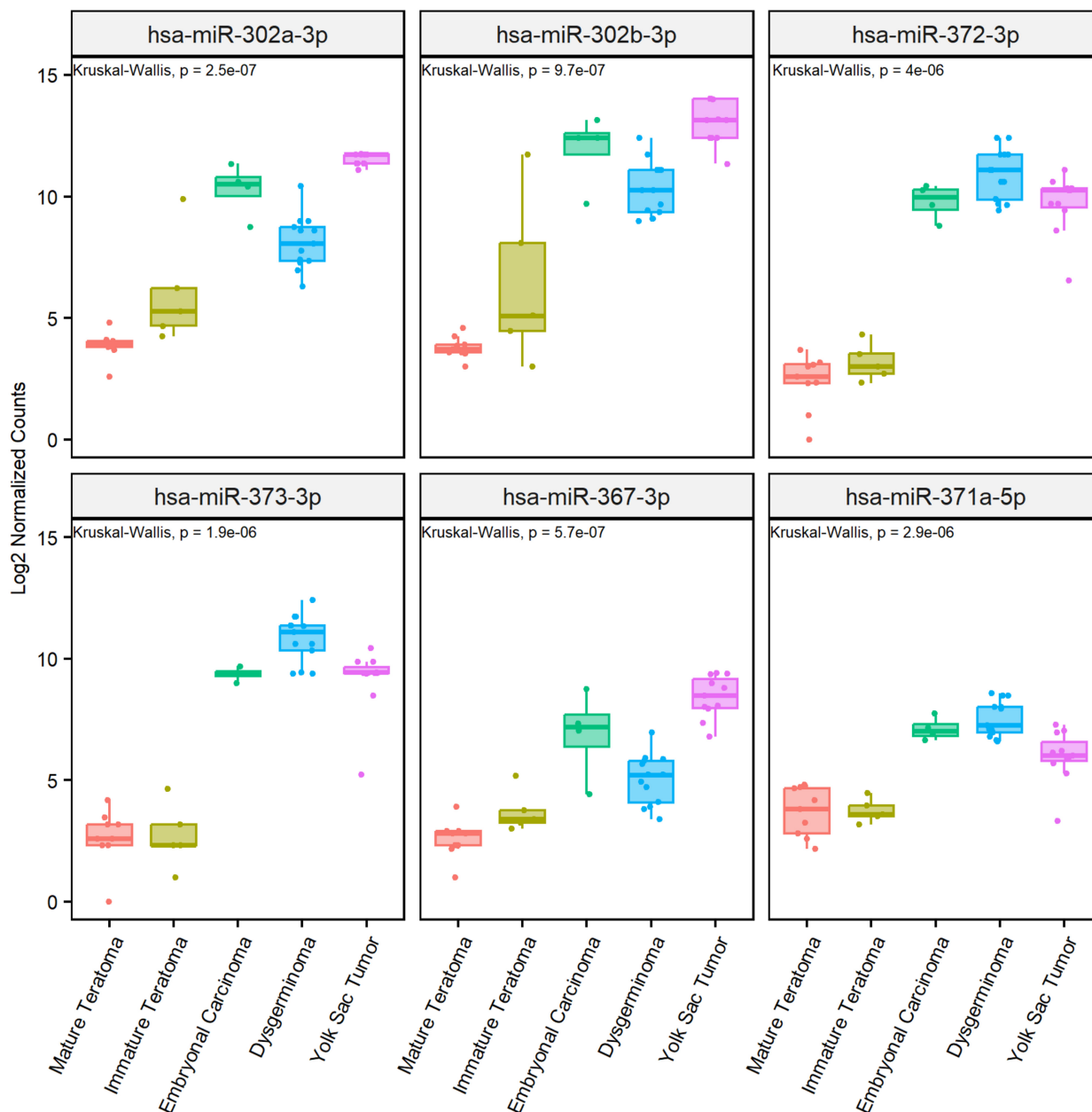


**Fig. 3.** miRNA expression levels in different histological types of pediatric GCT patients. Box-plot expression of miR-302a-3p, miR-302b-3p, miR-372-3p, miR-373-3p, miR-367-3p, and miR-371a-5p in dysgerminoma ( $n = 13$ ), embryonal carcinoma ( $n = 4$ ), mature ( $n = 7$ ) and immature teratomas ( $n = 5$ ), and yolk sac tumors ( $n = 11$ ).

dysgerminomas; miR-517b-3p, miR-1323, miR-525-5p, and miR-99b-5p were associated with EC; and miR-199a-5p, miR-199b-5p, miR-125b-5p, and let-7c/e were associated with immature teratomas.

Since each histology presented a signature of miRNAs, we investigated whether this signature could change according to the primary location of the tumor. Therefore, we evaluated the common and

specific miRNAs between the ovary and testis (Fig. 6, Table S4). We identified 20 miRNAs specific to testicular tumors (11 miRNAs upregulated and nine downregulated) and 18 to ovarian tumors (six miRNAs upregulated and 12 downregulated). In addition, 31 differentially expressed miRNAs were in common between the ovary and testis, in which the six miRNAs (miR-302a-3p, miR-302b-3p, miR-367-3p,

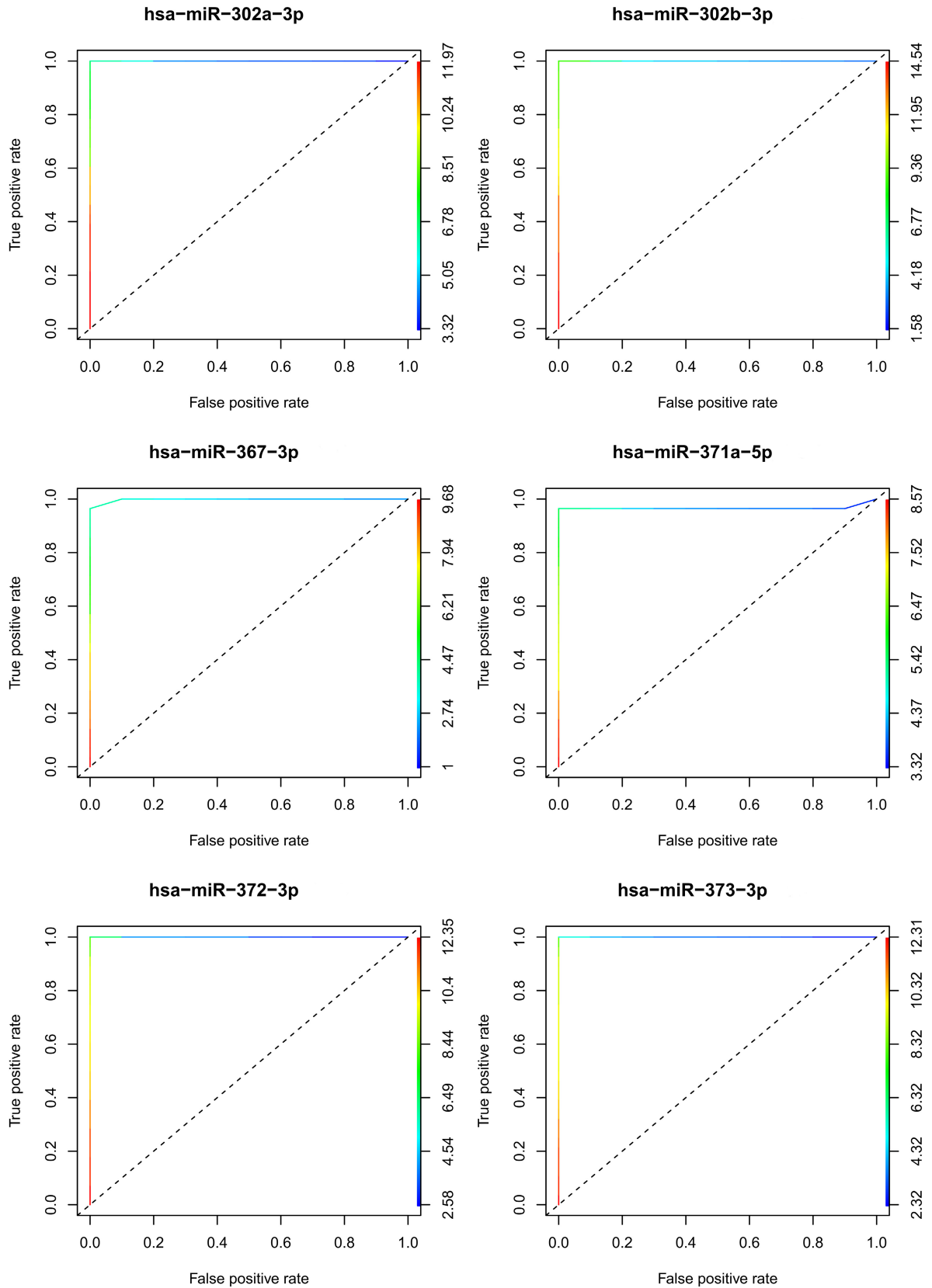




**Fig. 4.** Individual ROC curves for differentially expressed miRNAs in pediatric GCT patients. ROC curves show the performance of the six miRNAs in malignant GCTs (embryonal carcinoma, yolk sac tumor, dysgerminoma, and immature teratoma), including miR-302a-3p, miR-302b-3p, miR-367-3p, miR-371a-5p, miR-372-3p, and miR-373-3p. AUC, area under the curve and ROC, receiver operating characteristic.

miR-371a-5p, miR-372-3p, and miR-373-3p) were the most upregulated.

#### 4. Discussion

In the present study, miRNA expression was analyzed in a series of pediatric patients with gonadal GCTs. Initially, we identified differentially expressed miRNAs that could determine a specific signature of different histological types of GCTs, irrespective of the primary site (ovary or testicle). Furthermore, we identified miRNAs that were commonly expressed in malignant tumors and exhibited significant associations with the clinical features evaluated.

The age distribution of the patients in our study aligns with previous studies on pediatric GCTs, which exhibit a bimodal distribution with peaks in children under 5 years of age and in adolescence [23]. Yolk sac tumors and teratomas, or a combination of these two tumors (mixed tumors), are more frequent in younger children, while seminomas/dysgerminomas are predominant in pubertal and young adult patients [4]. Our results also showed patient relapse percentages consistent with the European Association of Urology (EAU) guidelines for testicular cancer, in which 15–30% of patients with TGCTs will relapse after first-line chemotherapy and require additional therapies. The low number of cancer-related deaths in our series is consistent with the high overall survival rate of GCTs, which is above 90% [24].

Evaluating the miRNA expression profiles in cancer may allow insights into tumorigenesis pathways since tumors present specific miRNA signatures [25]. The potential of miRNA expression as a tool to assist the diagnosis, prognosis, and management of patients with GCTs has been reported [13,26,27]. However, most studies are not specific to pediatric patients. Here, we analyzed 42 pediatric patients with GCTs, including primary tumors from ovaries and testicles, and different histological types. In this study, we excluded cases of mixed tumors to focus on identifying specific miRNA signatures for each histological type. In our preliminary analysis, as expected, the mature teratoma clustered with healthy control samples, indicating that patients with mature teratomas have similar molecular profiles of controls and may explain the fact that they are usually asymptomatic and have an overall good prognosis [28,29]. All mature teratoma samples in our

study were ovarian tumors, and previous studies have described that teratoma outside of the ovary is rare, and mature cystic teratoma is the most common GCT occurring in the ovary (90% in premenarchal girls and 60% in individuals younger than 20 years old) [28,29]. Furthermore, we showed that malignant histological types were grouped according to their miRNA expression profile, regardless of the primary site, suggesting that miRNA expression may be associated with the aggressive behavior of each GCT histological type.

Although we found an overlap of 26 miRNAs in the malignant tumors (yolk sac tumor, dysgerminoma, embryonal carcinoma, and immature teratoma), only six miRNAs were overexpressed (miR-302a-3p, miR-302b-3p, miR-371a-5p, miR-372-3p, miR-373-3p, and miR-367-3p). Notably, miR-302b-3p showed a significant correlation with all the evaluated clinical features, followed by miR-302a-3p, except for metastasis. Similar results were reported by Palmer et al., which demonstrated that the miR-371~373 and miR-302 clusters were differentially expressed regardless of histological subtype, site, or patient age [13]. Another study identified the miR-371~373 and miR-302 clusters as potential serum markers for malignant GCTs [30]. Special emphasis has been placed on the miRNA-371a-3p, which in a multicentric study has shown high sensitivity and specificity in the serum of patients with TGCTs, with an area under the curve (AUC) of 0.96 [31,32]. In addition, circulating miR-371a-3p was suggested as a biomarker for adult patients with TGCT prior to orchiectomy [15]. All these data support the use of miR-371a-3p in GCT patients, especially in adults with TGCTs. Interestingly, our results suggest that for pediatric patients with GCT, regardless of the primary tumor location, the miR-302a-3p and miR-302b-3p present greater importance and potential as biomarkers. The evaluation of the standard tumor markers AFP and HCG in malignant GCTs is limited due to their restricted sensitivity and specificity, and a significant number of patients will be negative for these markers. Thus, it is important to identify specific differentially expressed miRNAs for each histological type. In our study, we found 34 miRNAs specific for dysgerminomas when compared with healthy control samples, 13 miRNAs specific to EC, 25 miRNAs specific to YST, and one miRNA specific to immature teratoma. This is the first time that a comprehensive list of differentially expressed miRNAs has been described

**Table 3.** Correlation between differentially expressed miRNAs and clinical features of pediatric GCT patients with yolk sac tumor, dysgerminoma, and embryonal carcinoma. AFP, alpha-fetoprotein; GCTs, germ cell tumors; Max, maximum; Min, minimum.

Feature	hsa-miR-302a-3p		hsa-miR-302b-3p		hsa-miR-367-3p		hsa-miR-371a-5p		hsa-miR-372-3p		hsa-miR-373-3p	
	Median (min; max)	P value	Median (min; max)	P value	Median (min; max)	P value	Median (min; max)	P value	Median (min; max)	P value	Median (min; max)	P value
Histology												
Yolk sac tumor	11.8 (11.1; 11.8)	< <b>0.001<sup>a</sup></b>	13.3 (11.5; 13.8)	< <b>0.001<sup>a</sup></b>	8.5 (6.7; 9.5)	< <b>0.001<sup>a</sup></b>	5.8 (3.3; 7.3)	< <b>0.001<sup>a</sup></b>	10.1 (6.5; 11.1)	0.061 <sup>a</sup>	9.5 (5.1; 10.5)	< <b>0.001<sup>a</sup></b>
Embryonal carcinoma	10.3 (2.3; 4.6)		11.6 (9.6; 13.1)		7.3 (4.2; 8.5)		7.1 (6.6; 7.8)		9.6 (8.7; 10.3)		9.3 (8.8; 9.6)	
Mature teratoma	3.7 (2.3; 4.6)		3.6 (3.0; 4.5)		–		3.5 (2.0; 4.7)		–		–	
Immature teratoma	5.1 (4.3; 9.9)		5.0 (3.0; 11.6)		3.4 (2.5; 5.0)		–		–		2.5 (0; 4.6)	
Dysgerminoma	7.9 (6.2; 10.3)		9.9 (8.7; 11.7)		5.1 (3.4; 6.9)		7.2 (6.5; 8.3)		10.9 (9.5; 11.6)		10.9 (9.4; 11.6)	
Risk												
Low	4.6 (2.3; 11.8)	<b>0.050<sup>a</sup></b>	5.0 (3.0; 13.7)	<b>0.041<sup>a</sup></b>	6.1 (2.5; 8.9)	0.854 <sup>a</sup>	5.1 (2.0; 7.8)	< <b>0.001<sup>a</sup></b>	10.1 (8.5; 11.6)	0.642 <sup>a</sup>	9.5 (0; 11.4)	0.732 <sup>a</sup>
Intermediate	9.3 (6.2; 11.5)		11.5 (8.2; 13.3)		5.4 (3.8; 9.3)		7.6 (5.9; 7.9)		10.1 (9.7; 11.4)		9.5 (3.1; 11.2)	
High	8.6 (5.1; 11.8)		10.9 (4.3; 13.7)		5.8 (3.4; 9.5)		7.0 (3.3; 8.3)		10.5 (6.5; 11.6)		9.9 (2.5; 11.6)	
Metastasis												
Yes	10.1 (5.1; 11.8)	0.128 <sup>b</sup>	11.2 (4.4; 13.3)	< <b>0.001<sup>b</sup></b>	6.3 (3.4; 9.5)	0.603 <sup>b</sup>	7.1 (3.3; 8.3)	0.073 <sup>b</sup>	10.3 (6.5; 11.6)	0.784 <sup>b</sup>	9.5 (2.5; 11.6)	0.802 <sup>b</sup>
No	7.8 (2.3; 11.8)		9.5 (3.0; 13.8)		5.7 (2.5; 9.4)		5.9 (2.0; 8.2)		10.2 (8.5; 11.6)		9.5 (0; 11.4)	
AFP pre surgical												
Normal	6.8 (2.3; 11.8)	<b>0.001<sup>b</sup></b>	8.8 (3.0; 12.6)	< <b>0.001<sup>b</sup></b>	5.1 (3.1; 7.9)	<b>0.002<sup>b</sup></b>	6.5 (2.0; 8.3)	0.711 <sup>b</sup>	10.8 (6.5; 11.6)	0.573 <sup>b</sup>	10.9 (2.5; 11.6)	0.351 <sup>b</sup>
Increased	11.6 (6.9; 11.8)		13.3 (9.6; 13.7)		8.2 (5.6; 9.5)		5.9 (5.5; 7.3)		10.2 (9.5; 11.1)		9.5 (9.4; 10.5)	
Relapse												
No	7.7 (2.3; 11.8)	<b>0.016<sup>b</sup></b>	9.6 (3.0; 13.7)	<b>0.029<sup>b</sup></b>	5.6 (2.5; 9.5)	0.116 <sup>b</sup>	6.6 (2.2; 8.3)	> 0.999 <sup>b</sup>	10.3 (6.5; 11.6)	0.413 <sup>b</sup>	9.5 (0; 11.6)	0.942 <sup>b</sup>
Yes	11.5 (8.5; 11.8)		12.6 (9.6; 13.7)		7.9 (4.2; 9.4)		5.9 (5.1; 7.8)		10.1 (8.5; 11.1)		9.5 (8.5; 10.5)	
Status												
Alive	7.9 (2.3; 11.8)	<b>0.009<sup>b</sup></b>	9.6 (3.0; 13.7)	<b>0.036<sup>b</sup></b>	5.6 (2.5; 9.5)	0.115 <sup>b</sup>	6.7 (2.0; 8.3)	0.202 <sup>b</sup>	10.3 (8.7; 11.6)	0.219 <sup>b</sup>	9.5 (0; 11.6)	0.491 <sup>b</sup>
Dead	11.8 (11.5; 11.8)		12.6 (12.6; 13.7)		7.9 (6.7; 9.4)		5.1 (3.3; 5.9)		8.5 (6.5; 11.1)		8.5 (5.1; 10.5)	

<sup>a</sup>Kruskal–Wallis test.

<sup>b</sup>Mann–Whitney test.

All numbers in bold are events that had significance with a P value < 0.05, according to the Materials and Methods section, item 2.4 statistical analysis.

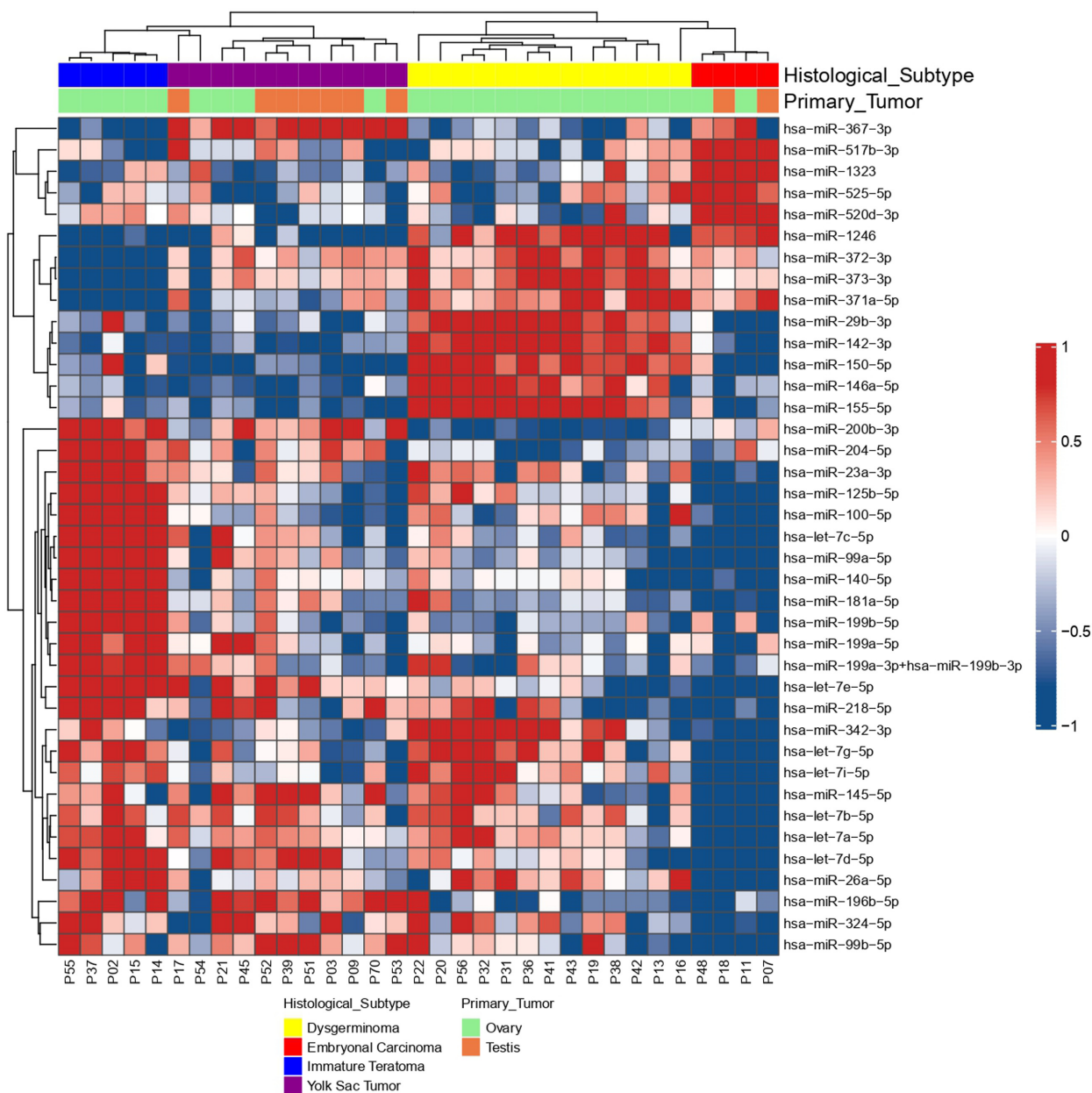


**Fig. 5.** Heatmap and dendrogram of differentially expressed miRNAs in different histological types. Expression levels were used to group miRNA profiles according to their similarities between histological types, including embryonal carcinoma (red), dysgerminoma (yellow), yolk sac tumor (purple), and immature teratoma (blue). The heatmap shows a distinct miRNA expression profile in the four groups studied. Rows indicate the relative expression levels for a single miRNA, and columns indicate the expression level for a single sample. Blue and red colors indicate the miRNAs with lower and higher expression levels, respectively.

for each histological type of GCTs. In the immature teratoma analysis, miR-199b-5p was overexpressed, and similar results were reported in pediatric intracranial GCTs [33]. In medulloblastoma, miR-199b-5p was associated with metastasis [34]. Most of the miRNAs identified in our study were overexpressed in tumor tissues, except for EC, which presented only one miRNA

upregulated (miR-1323) and 12 were downregulated. To the best of our knowledge, miR-1323 has not been previously reported in GCTs, although it has been associated with tumor progression in hepatocellular carcinoma [35], migration in lung adenocarcinoma [36], and breast cancer [37]. The top five highly expressed miRNAs in YST were miR-122-5p, miR-200c-3p,

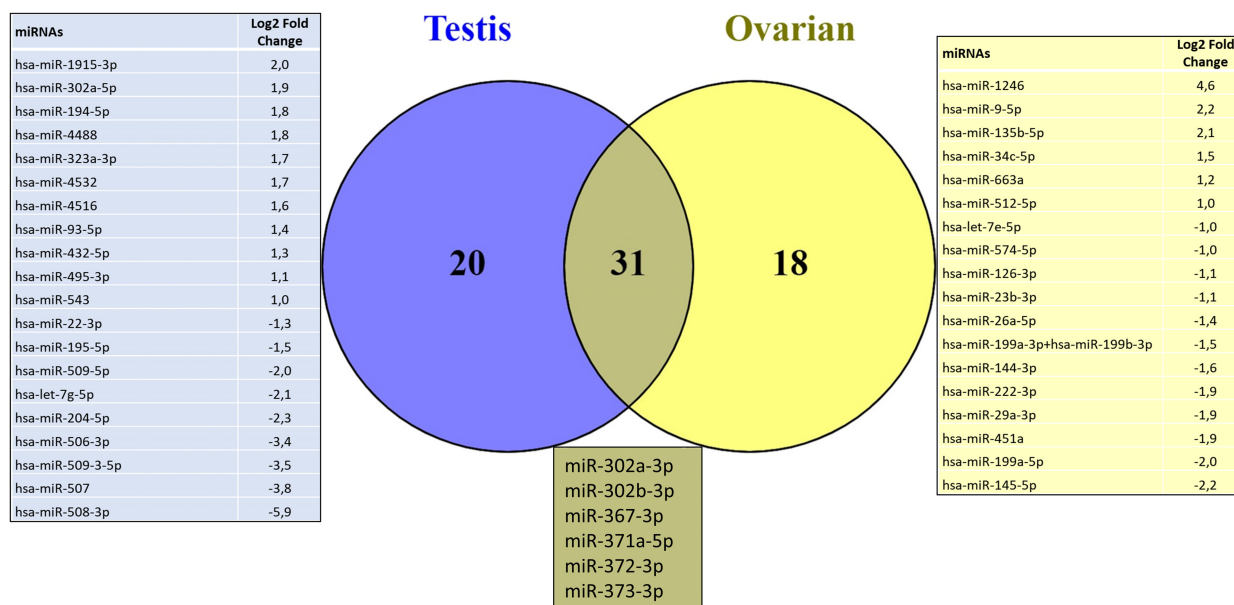


**Fig. 6.** Venn diagram shows miRNA distribution among the testis and ovarian tumors. Venn diagrams indicate the number of significant differentially expressed miRNAs in testis (20 miRNAs) and ovarian (18 miRNAs) tumors, and the overlap regions show the number of miRNAs expressed in two tumors.

miR-302a-5p, hsa-miR-323a-3p, and miR-141-3p. None of these miRNAs have been previously described in GCTs, but they play important roles in nephroblastoma [38], melanoma [39], lung tumors [40], and colorectal cancer [41]. In dysgerminomas, the top five overexpressed miRNAs were miR-142-3p, miR-146a-5p, miR-21-5p, miR-182-5p, and miR-223-3p. The upregulation of miR-142-3p [42], miR-182-5p [43], and miR-223-3p [44] has been previously shown in TGCTs. In addition, the increased expression of miR-146a-5p and miR-21-5p has been correlated with other cancer types, including breast [45], penile [46], and prostate [47], but not with GCTs.

We examined whether alterations in the miRNA signature were associated with the primary site of the tumor, we identified 20 miRNAs specific to testicular tumor and 18 miRNAs specific to ovarian tumors, and 31 differentially expressed miRNAs were in common between the ovary and testis. Among the 31 miRNAs, it included the six miRNAs upregulated in YST, EC, and dysgerminomas (miR-302a-3p, miR-302b-3p, miR-367-3p, miR-371a-5p, miR-372-3p, and miR-373-3p), suggesting that GCTs have similar histological pattern independent of their primary site [48].

The lack of longitudinal follow-up in our study limits the analysis of miRNA levels in recurrent cases. In addition, we focused on gonadal tumors (ovarian and testicle) since it is more frequent and on five histological types (YST, dysgerminoma, EC, and mature

and immature teratoma). We did not have samples to represent choriocarcinoma and seminoma histologies. We excluded mixed GCT samples because it is difficult to make a comprehensive evaluation of this tumor as a whole, and microdissection is more recommended. Therefore, further studies involving other primary tumor locations and histological types, including testicular seminoma, choriocarcinoma, and mixed GCTs, are needed.

The findings of our study are consistent with previous evidence pointing to miRNAs as potential biomarkers in pediatric GCTs. Our results indicate that the signature of miRNAs for each histological type may be useful as a standard clinical assessment to help with the diagnosis, prognosis, and management of GCT patients, but further studies are necessary to validate our findings.

## 5. Conclusions

We report that miRNA expression profiles are associated with histological types of pediatric gonadal GCTs, regardless of the primary site. Yolk sac tumor, dysgerminoma, embryonal carcinoma, and immature teratoma showed an overlap of these six miRNAs miR-302b-3p, miR-302a-3p, miR-372-3p, miR-373-3p, miR-367-3p, and miR-371a-5p, suggesting their clinical value for the management of pediatric patients with malignant GCTs. Our results highlight the differentially expressed

miRNAs for each histological type, demonstrating the potential for microRNA expression to assist the diagnosis, prognostic, and management of patients with malignant GCTs.

## Acknowledgements

We gratefully thank the Public Ministry of Labor of Campinas (Research, Prevention and Education of Occupational Cancer — zone 15<sup>a</sup>, Campinas, Brazil), the São Paulo State Research Support Foundation (FAPESP - Process n. 2019/07502-8) and the internal program of resources for research of the Barretos Cancer Hospital (PAIP) for funding this study.

## Conflict of interest

The authors declare no conflict of interest.

## Author contributions

AGSV: Conceptualization, Data curation, Formal analysis, Investigation, Methodology, Resources, Software, Visualization, Writing—original draft. LSS: Methodology, Software, Validation, Writing—review & editing. ECAS: Data curation, Methodology, Investigation, Writing—review & editing. ACL: Investigation, Methodology, Writing—review & editing. TMVF: Data curation, Writing—review & editing. AHL: Investigation, Methodology, Writing—review & editing. GEM: Conceptualization, Data curation, Writing—review & editing. MAO: Formal analysis, Methodology, Validation, Writing—review & editing. RMR: Funding acquisition, Investigation, Methodology, Resources, Validation, Writing—review & editing. LFL: Conceptualization, Investigation, Methodology, Project administration, Resources, Supervision, Validation, Writing—review & editing. MTP: Conceptualization, Formal analysis, Investigation, Methodology, Project administration, Resources, Supervision, Validation, Writing—original draft, Writing—review & editing.

## Peer review

The peer review history for this article is available at <https://www.webofscience.com/api/gateway/wos/peer-review/10.1002/1878-0261.13617>.

## Data accessibility

The datasets analyzed in the current study are available from the corresponding author upon reasonable request.

## References

- Schneider DT, Calaminus G, Koch S, Teske C, Schmidt P, Haas RJ, et al. Epidemiologic analysis of 1,442 children and adolescents registered in the German germ cell tumor protocols. *Pediatr Blood Cancer*. 2004;**42**:169–75. <https://doi.org/10.1002/pbc.10321>
- Pierce JL, Frazier AL, Amatruda JF. Pediatric germ cell tumors: a developmental perspective. *Ther Adv Urol*. 2018;**2018**:1–8. <https://doi.org/10.1155/2018/9059382>
- Becker C, Graf N, Grabow D, Creutzig U, Reinhardt D, Weyer-Elberich V, et al. Early deaths from childhood cancer in Germany 1980–2016. *Cancer Epidemiol*. 2020;**65**:101669. <https://doi.org/10.1016/j.canep.2020.101669>
- Robert J, Kurman MLC, Simon Herrington C, Robert HY. WHO classification of tumours of female reproductive organs. 4th ed. Lyon, France: International Agency for Research on Cancer (IARC); 2014.
- Charytonowicz D, Aubrey H, Bell C, Ferret M, Tsui K, Atfield R, et al. Cost analysis of noninvasive blood-based microRNA testing versus CT scans for follow-up in patients with testicular germ-cell tumors. *Clin Genitourin Cancer*. 2019;**17**:e733–44. <https://doi.org/10.1016/j.clgc.2019.03.015>
- Dieckmann K-P, Simonsen-Richter H, Kulejewski M, Anheuser P, Zecha H, Isbarn H, et al. Serum tumour markers in testicular germ cell tumours: frequencies of elevated levels and extents of marker elevation are significantly associated with clinical parameters and with response to treatment. *Biomed Res Int*. 2019;**2019**:1–22. <https://doi.org/10.1155/2019/5030349>
- Horwich A, Shipley J, Huddart R. Testicular germ-cell cancer. *Lancet*. 2006;**367**:754–65. [https://doi.org/10.1016/S0140-6736\(06\)68305-0](https://doi.org/10.1016/S0140-6736(06)68305-0)
- von Eyben FE. Lactate dehydrogenase isoenzyme 1 is the most important LD isoenzyme in patients with testicular germ cell tumor. *Acta Oncol*. 2000;**39**:509–17. <https://doi.org/10.1080/028418600750013438>
- Bonfig W, Hempel M, Teichert-von Lutichau I, Liptay S, Burdach S. Avoiding harmful procedures in patients with elevated alpha-fetoprotein concentrations: hereditary persistence of alpha-fetoprotein is an important and benign differential diagnosis. *J Pediatr Hematol Oncol*. 2012;**34**(7):e301–3.
- Shivdasani RA. microRNAs: regulators of gene expression and cell differentiation. *Blood*. 2006;**108**:3646–53. <https://doi.org/10.1182/blood-2006-01-030015>
- Das MK, Evensen HSF, Furu K, Haugen TB. miRNA-302s may act as oncogenes in human testicular germ cell tumours. *Sci Rep*. 2019;**9**:9189. <https://doi.org/10.1038/s41598-019-45573-6>

- 12 Almeida MI, Reis RM, Calin GA. microRNA history: discovery, recent applications, and next frontiers. *Mutat Res.* 2011;**717**:1–8. <https://doi.org/10.1016/j.mrfmmm.2011.03.009>
- 13 Palmer RD, Murray MJ, Saini HK, van Dongen S, Abreu-Goodger C, Muralidhar B, et al. Malignant germ cell tumors display common microRNA profiles resulting in global changes in expression of messenger RNA targets. *Cancer Res.* 2010;**70**:2911–23. <https://doi.org/10.1158/0008-5472.CAN-09-3301>
- 14 Syring I, Bartels J, Holdenrieder S, Kristiansen G, Müller SC, Ellinger J. Circulating serum miRNA (miR-367-3p, miR-371a-3p, miR-372-3p and miR-373-3p) as biomarkers in patients with testicular germ cell cancer. *J Urol.* 2015;**193**:331–7. <https://doi.org/10.1016/j.juro.2014.07.010>
- 15 Badia RR, Abe D, Wong D, Singla N, Savelyeva A, Chertack N, et al. Real-world application of pre-orchiectomy miR-371a-3p test in testicular germ cell tumor management. *J Urol.* 2021;**205**:137–44. <https://doi.org/10.1097/JU.0000000000001337>
- 16 Lopes LF. Protocolo TCG-GALOP-2017: tumores de células germinativas da infância e adolescência. São Paulo, Brazil: Lemar; 2018.
- 17 Evangelista AF, Zanon MF, Carloni AC, de Paula FE, Morini MA, Ferreira-Neto M, et al. Detection of ALK fusion transcripts in FFPE lung cancer samples by NanoString technology. *BMC Pulm Med.* 2017;**17**:86. <https://doi.org/10.1186/s12890-017-0428-0>
- 18 Pessôa-Pereira D, Evangelista AF, Causin RL, da Costa Vieira RA, Abrahão-Machado LF, Santana IVV, et al. miRNA expression profiling of hereditary breast tumors from BRCA1- and BRCA2-germline mutation carriers in Brazil. *BMC Cancer.* 2020;**20**:143. <https://doi.org/10.1186/s12885-020-6640-y>
- 19 Waggott D, Chu K, Yin S, Wouters BG, Liu F-F, Boutros PC. NanoStringNorm: an extensible R package for the pre-processing of NanoString mRNA and miRNA data. *Bioinformatics.* 2012;**28**:1546–8. <https://doi.org/10.1093/bioinformatics/bts188>
- 20 Gu Z, Eils R, Schlesner M. Complex heatmaps reveal patterns and correlations in multidimensional genomic data. *Bioinformatics.* 2016;**32**:2847–9. <https://doi.org/10.1093/bioinformatics/btw313>
- 21 van der Maaten L. Accelerating t-SNE using tree-based algorithms. *J Mach Learn Res.* 2014;**15**:3221–45.
- 22 van der Maaten L, Hinton G. Visualizing data using t-SNE. *J Mach Learn Res.* 2008;**9**:2579–605.
- 23 Poynter JN, Amatruda JF, Ross JA. Trends in incidence and survival of pediatric and adolescent patients with germ cell tumors in the United States, 1975 to 2006. *Cancer.* 2010;**116**:4882–91. <https://doi.org/10.1002/cncr.25454>
- 24 Siegel RL, Miller KD, Jemal A. Cancer statistics, 2020. *CA Cancer J Clin.* 2020;**70**:7–30. <https://doi.org/10.3322/caac.21590>
- 25 Nagalla S, Chou JW, Willingham MC, Ruiz J, Vaughn JP, Dubey P, et al. Interactions between immunity, proliferation and molecular subtype in breast cancer prognosis. *Genome Biol.* 2013;**14**:R34. <https://doi.org/10.1186/gb-2013-14-4-r34>
- 26 Voorhoeve PM, le Sage C, Schrier M, Gillis AJM, Stoop H, Nagel R, et al. A genetic screen implicates miRNA-372 and miRNA-373 As oncogenes in testicular germ cell tumors. *Cell.* 2006;**124**:1169–81. <https://doi.org/10.1016/j.cell.2006.02.037>
- 27 Gillis A, Stoop H, Hersmus R, Oosterhuis J, Sun Y, Chen C, et al. High-throughput microRNAome analysis in human germ cell tumours. *J Pathol.* 2007;**213**:319–28. <https://doi.org/10.1002/path.2230>
- 28 Green DB, La Rosa FG, Craig PG, Khani F, Lam ET. Metastatic mature teratoma and growing teratoma syndrome in patients with testicular non-Seminomatous germ cell tumors. *Korean J Radiol.* 2021;**22**:1650–7. <https://doi.org/10.3348/kjr.2020.1391>
- 29 Euscher ED. Germ cell tumors of the female genital tract. *Surg Pathol Clin.* 2019;**12**:621–49. <https://doi.org/10.1016/j.path.2019.01.005>
- 30 Murray MJ, Halsall DJ, Hook CE, Williams DM, Nicholson JC, Coleman N. Identification of microRNAs from the miR-371 ~ 373 and miR-302 clusters as potential serum biomarkers of malignant germ cell tumors. *Am J Clin Pathol.* 2011;**135**:119–25. <https://doi.org/10.1309/AJCPOE11KEYZCJHT>
- 31 Dieckmann K-P, Radtke A, Geczi L, Matthies C, Anheuser P, Eckardt U, et al. Serum levels of microRNA-371a-3p (M371 test) as a new biomarker of testicular germ cell tumors: results of a prospective multicentric study. *J Clin Oncol.* 2019;**37**:1412–23. <https://doi.org/10.1200/JCO.18.01480>
- 32 Kulkarni MM. Digital multiplexed gene expression analysis using the NanoString nCounter system. *Curr Protoc Mol Biol.* 2011;**Chapter 25**:Unit25B.10. <https://doi.org/10.1002/0471142727.mb25b10s94>
- 33 Hsieh TH, Liu YR, Chang TY, Liang ML, Chen HH, Wang HW, et al. Global DNA methylation analysis reveals miR-214-3p contributes to cisplatin resistance in pediatric intracranial nongerminomatous malignant germ cell tumors. *Neuro-Oncology.* 2018;**20**:519–30. <https://doi.org/10.1093/neuonc/nox186>
- 34 Andolfo I, Liguori L, De Antonellis P, Cusanelli E, Marinaro F, Pistollato F, et al. The micro-RNA 199b-5p regulatory circuit involves Hes1, CD15, and epigenetic modifications in medulloblastoma. *Neuro-Oncology.* 2012;**14**:596–612. <https://doi.org/10.1093/neuonc/nos002>
- 35 Zhang F, Yang C, Xing Z, Liu P, Zhang B, Ma X, et al. LncRNA GAS5-mediated miR-1323 promotes tumor progression by targeting TP53INP1 in hepatocellular carcinoma. *Onco Targets Ther.* 2019;**12**:4013–23. <https://doi.org/10.2147/OTT.S209439>

- 36 Zhao H, Zheng C, Wang Y, Hou K, Yang X, Cheng Y, et al. miR-1323 promotes cell migration in lung adenocarcinoma by targeting Cbl-b and is an early prognostic biomarker. *Front Oncol.* 2020;**10**:181. <https://doi.org/10.3389/fonc.2020.00181>
- 37 Xu Y, Liu M. microRNA-1323 downregulation promotes migration and invasion of breast cancer cells by targeting tumour protein D52. *J Biochem.* 2020;**168**:83–91. <https://doi.org/10.1093/jb/mvaa035>
- 38 Li T, Zhao P, Li Z, Wang C-C, Wang Y-L, Gu Q. miR-200c-3p suppresses the proliferative, migratory, and invasive capacities of nephroblastoma cells via targeting FRS2. *Biopreserv Biobank.* 2019;**17**:444–51. <https://doi.org/10.1089/bio.2019.0009>
- 39 Byrnes CC, Jia W, Alshamrani AA, Kuppa SS, Murph MM. miR-122-5p expression and secretion in melanoma cells is amplified by the LPAR3 SH3-binding domain to regulate Wnt1. *Mol Cancer Res.* 2019;**17**:299–309. <https://doi.org/10.1158/1541-7786.MCR-18-0460>
- 40 Wang H-Y, Liu Y-N, Wu S-G, Hsu C-L, Chang T-H, Tsai M-F, et al. MiR-200c-3p suppression is associated with development of acquired resistance to epidermal growth factor receptor (EGFR) tyrosine kinase inhibitors in EGFR mutant non-small cell lung cancer via a mediating epithelial-to-mesenchymal transition (EMT) process. *Cancer Biomark.* 2020;**28**:351–63. <https://doi.org/10.3233/CBM-191119>
- 41 Ardila H, Sanabria-Salas M, Meneses X, Rios R, Huertas-Salgado A, Serrano M. Circulating miR-141-3p, miR-143-3p and miR-200c-3p are differentially expressed in colorectal cancer and advanced adenomas. *Mol Clin Oncol.* 2019;**11**:201–7. <https://doi.org/10.3892/mco.2019.1876>
- 42 Tanaka K, Kondo K, Kitajima K, Muraoka M, Nozawa A, Hara T. Tumor-suppressive function of protein-tyrosine phosphatase non-receptor type 23 in testicular germ cell tumors is lost upon overexpression of miR142-3p microRNA. *J Biol Chem.* 2013;**288**:23990–9. <https://doi.org/10.1074/jbc.M113.478891>
- 43 Mallik S, Qin G, Jia P, Zhao Z. Molecular signatures identified by integrating gene expression and methylation in non-seminoma and seminoma of testicular germ cell tumours. *Epigenetics.* 2021;**16**:162–76. <https://doi.org/10.1080/15592294.2020.1790108>
- 44 Liu J, Shi H, Li X, Chen G, Larsson C, Lui W-O. miR-223-3p regulates cell growth and apoptosis via FBXW7 suggesting an oncogenic role in human testicular germ cell tumors. *Int J Oncol.* 2017;**50**:356–64. <https://doi.org/10.3892/ijco.2016.3807>
- 45 Wei G, Jing H, Zhaoyang J, Jiping D, Zengwei H, Yun D, et al. Expression of miR-146a-5p in breast cancer and its role in proliferation of breast cancer cells. *Oncol Lett.* 2018;**15**:9884–8. <https://doi.org/10.3892/ol.2018.8589>
- 46 Pinho JD, Silva GEB, Teixeira Júnior AAL, Belfort MRC, Mendes JM, Cunha IWD, et al. MIR-107, MIR-223-3P and MIR-21-5P reveals potential biomarkers in penile cancer. *Asian Pac J Cancer Prev.* 2020;**21**:391–7. <https://doi.org/10.31557/APJCP.2020.21.2.391>
- 47 Danarto R, Astuti I, Umbas R, Haryana SM. Urine miR-21-5p and miR-200c-3p as potential non-invasive biomarkers in patients with prostate cancer. *Turk J Urol.* 2020;**46**:26–30.
- 48 Gobel U, Schneider DT, Calaminus G, Haas RJ, Schmidt P, Harms D. Germ-cell tumors in childhood and adolescence. *Ann Oncol.* 2000;**11**:263–71. <https://doi.org/10.1023/a:1008360523160>

## Supporting information

Additional supporting information may be found online in the Supporting Information section at the end of the article.

**Fig. S1.** Heatmap and dendrogram of differentially expressed miRNAs in pediatric malignant germ cell tumors.

**Fig. S2.** MicroRNA expression profile of each germ cell tumors histology when compared with control samples.

**Table S1.** List of 34 differentially expressed miRNAs in dysgerminomas compared with healthy control samples.

**Table S2.** List of 13 differentially expressed miRNAs in embryonal carcinoma compared with healthy control samples.

**Table S3.** List of 25 differentially expressed miRNAs in yolk sac tumors compared to healthy control samples.

**Table S4.** Overlap of 31 differentially expressed miRNAs in testicular and ovarian tumors.